Resolving the BLR with VLTI/GRAVITY

Daryl Joe Santos, Taro Shimizu, Jinyi Shangguan, Richard Davies,
Yixian Cao, Eckhard Sturm, Dieter Lutz, and the GRAVITY Collaboration

The Restless Nature of AGN @ University of Naples, Jun. 26-30, 2023

Resolving the BLR with GRAVITY

Very Large Telescope Interferometer (VLTI)

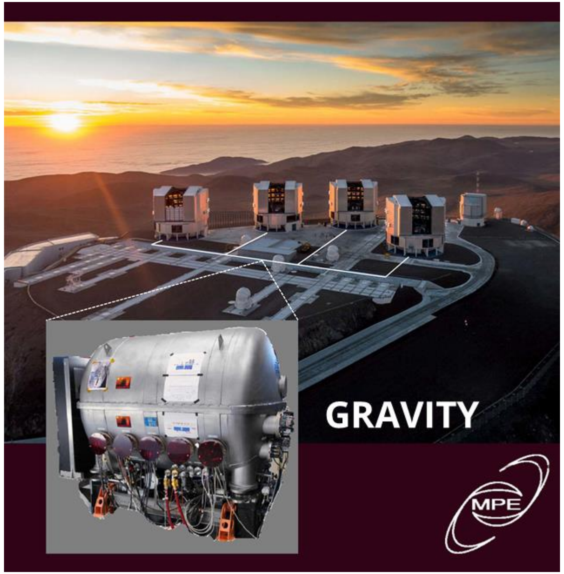

(c) MPE

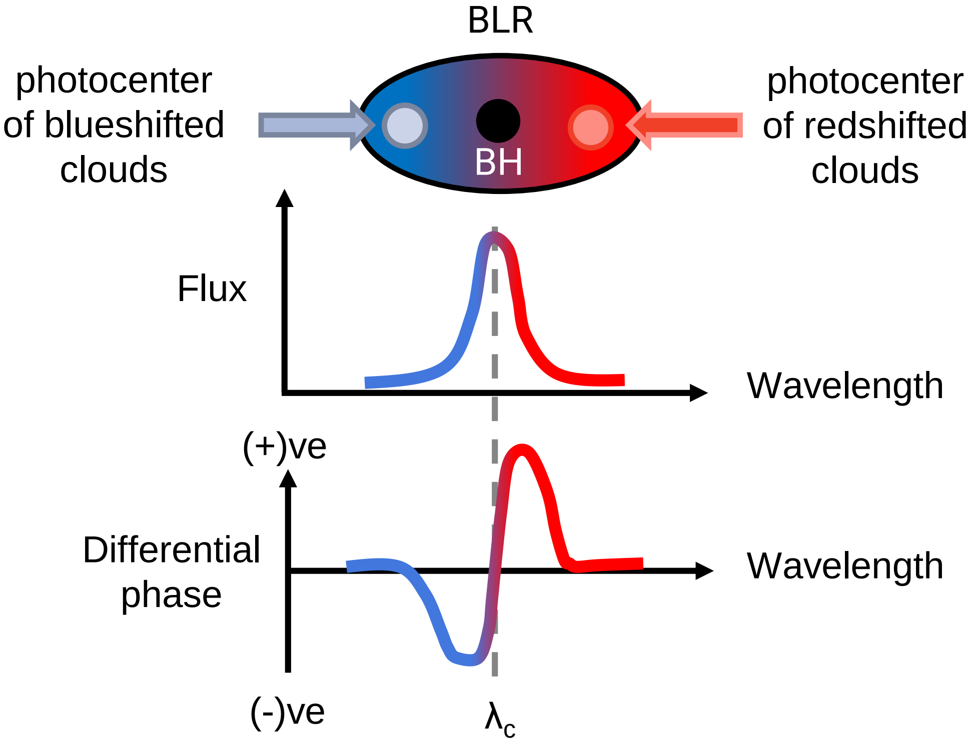

GRAVITY-AGN Project: Goals and Questions

Main goal: To directly measure **BLR structure and BH masses** with GRAVITY and view in the context of **AGN scaling relations (e.g., R-L relation)** previously derived by other methods.

Mrk 509

PDS 456

Mrk 1239

IC 4329A

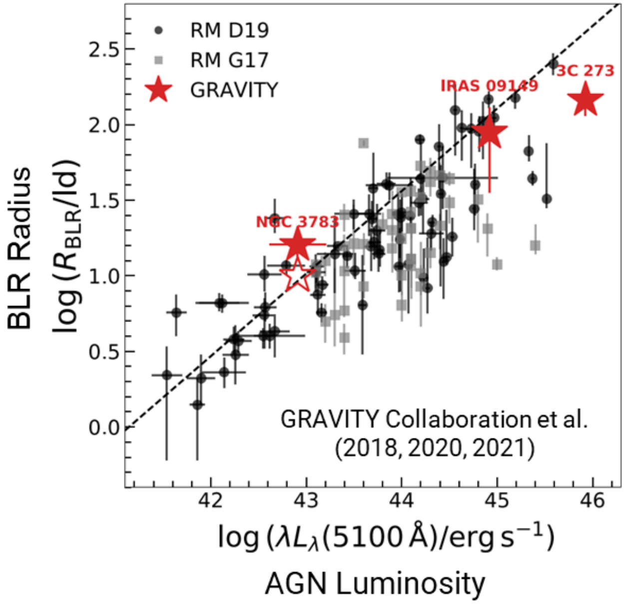

What can we learn about the BLRs of GRAVITY-observed AGNs?

Where do GRAVITY-observed AGNs lie in the R-L relation?

Ultimate goal: Investigate R-L relation, study AGNs, and measure BH masses at **higher redshift**

We have spatially resolved the BLRs of our 4 new targets

Photocenter fitting results, independent of any BLR models, indicate that we have spatially resolved their BLRs

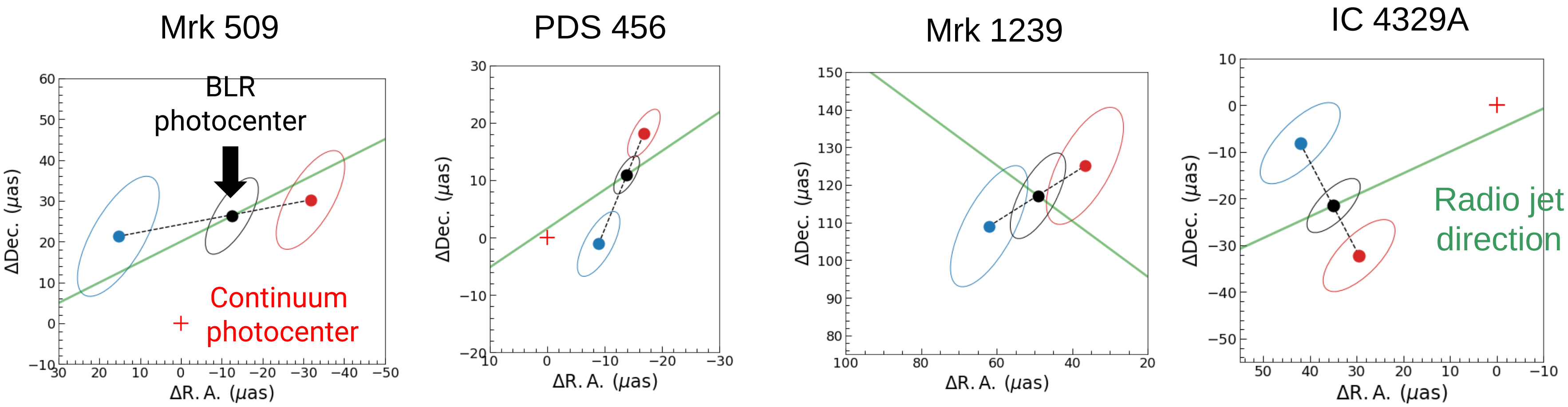

However, photocenter fitting is not enough!

BLR Model Fitting

BLR Model based on Pancoast+14

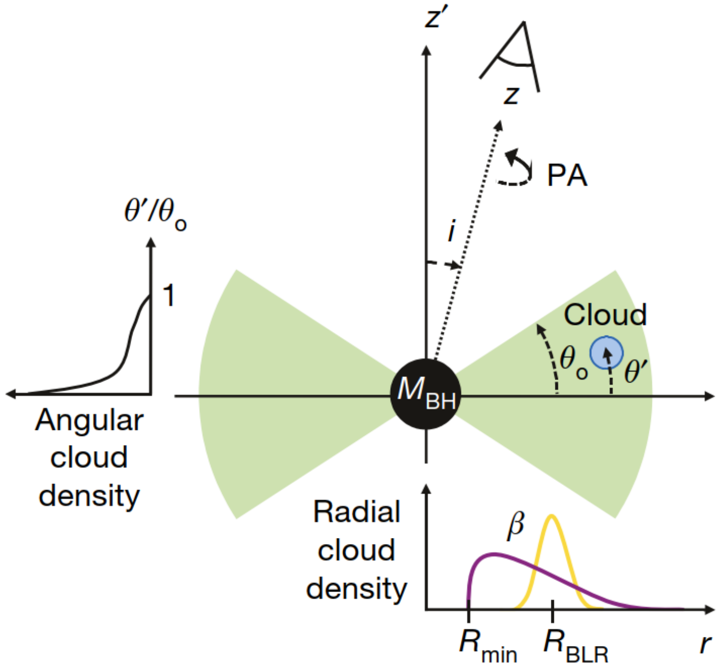

The BLR is a collection of non-interacting clouds encircling the central SMBH.

BLR radius
BH mass
Tangential and radial velocities of each cloud

Outflow-dominated BLRs

Mrk 1239, IC 4329A, 3C 273, NGC 3783, IRAS 09149-6206:
Keplerian-dominated BLR

© GRAVITY Collaboration et al. (2018)

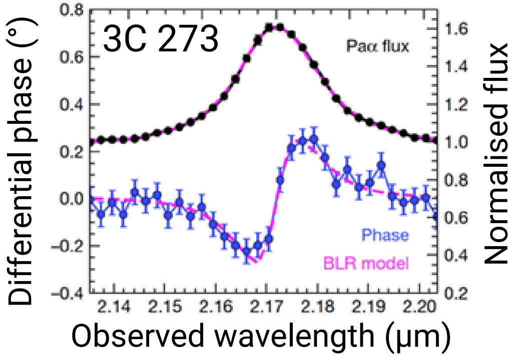

Mrk 509, PDS 456:
Outflow-dominated BLR

© GRAVITY Collaboration et al. (in prep.)

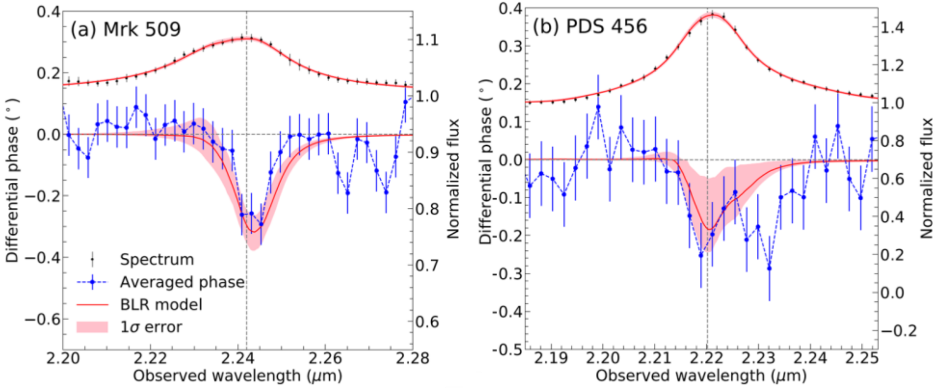

GRAVITY BLR sizes vs. Classical R-L relation from Bentz+13

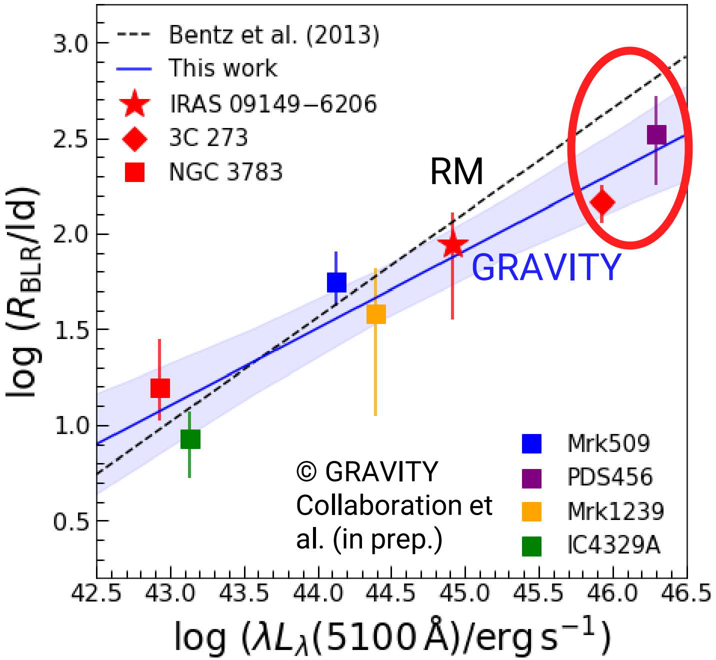

R-L relation:

Lower BLR sizes at higher luminosities

Conclusion similar to works using RM campaigns that find lower BLR sizes at higher luminosities and/or higher accretion rates (e.g., Du & Wang, 2019)

More luminous (more massive) AGNs more difficult to observe with RM due to longer observation periods

Virial Factors of GRAVITY-observed AGNs

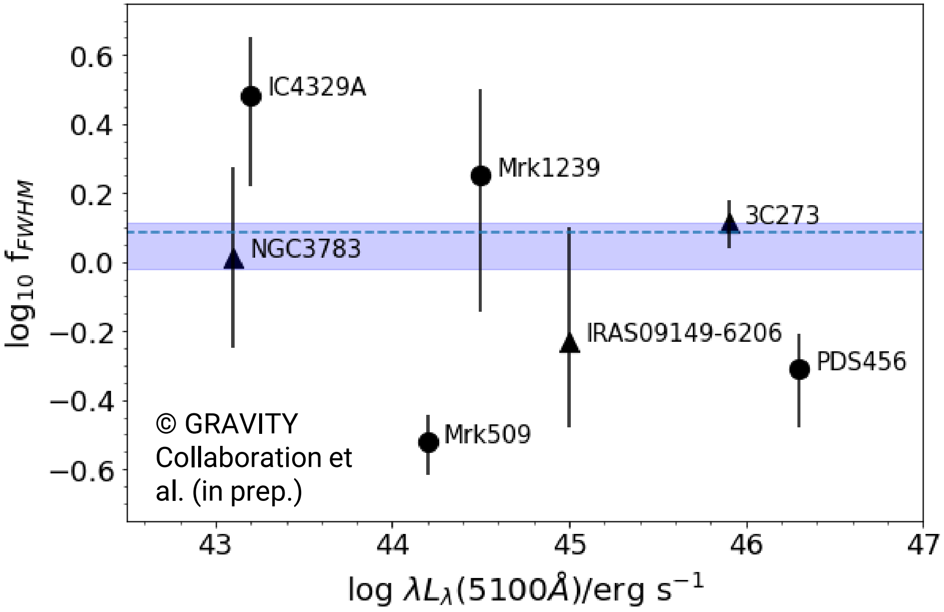

From GRAVITY observations

$$G M_{BH} = f_{FWHM} R_{BLR} (\Delta V)^2$$

$$< f_{FWHM} > = 1.26 \pm 0.28$$

Similar with previous works' <f> calculated by assuming evidence outside RM (e.g., AGNs following quiescent galaxies' M-σ relation) (e.g., Onken+04, Woo+10, Park+12)

Pearson correlation p-value ~ 0.3 → no significant trend

Observing z~2 quasars with GRAVITY Wide

Example:
LAMOST J0920+0657

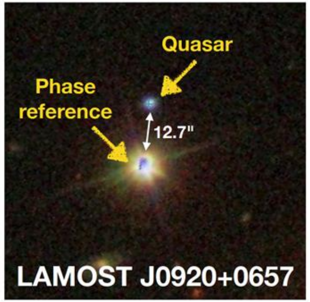

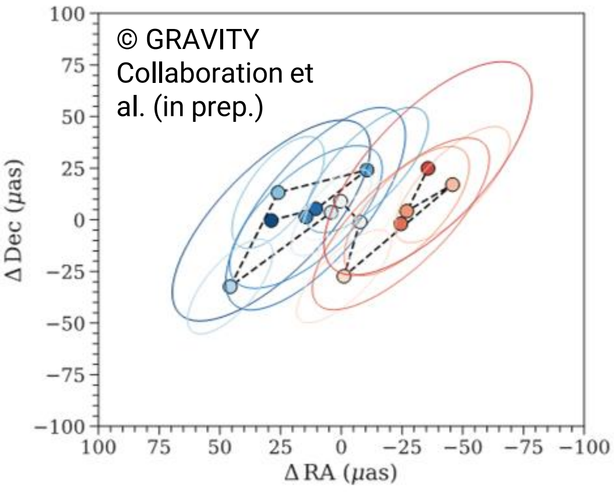

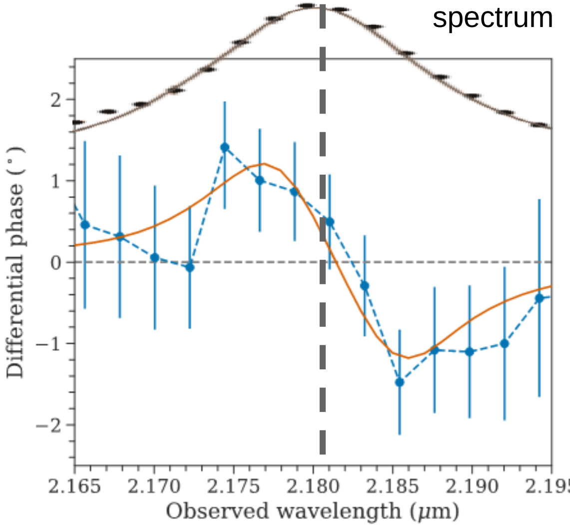

$$R_{BLR} = 40^{+20}_{-13}\ \mu as \sim 405\ ld$$

$$\log M_{BH} = 8.51^{+0.22}_{-0.23}\ M_{\odot}$$

Dynamical BH mass measurement of a z ~2 AGN with **~3 hours** of integration with GRAVITY, many more to come!

Location of LAMOST J0920 in the R-L Relation

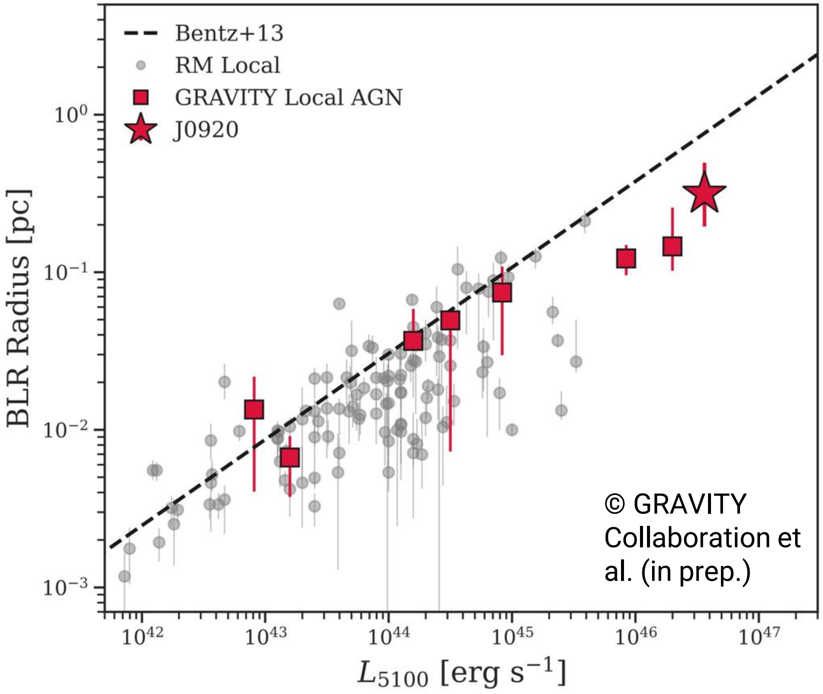

Future Prospects: GRAVITY+

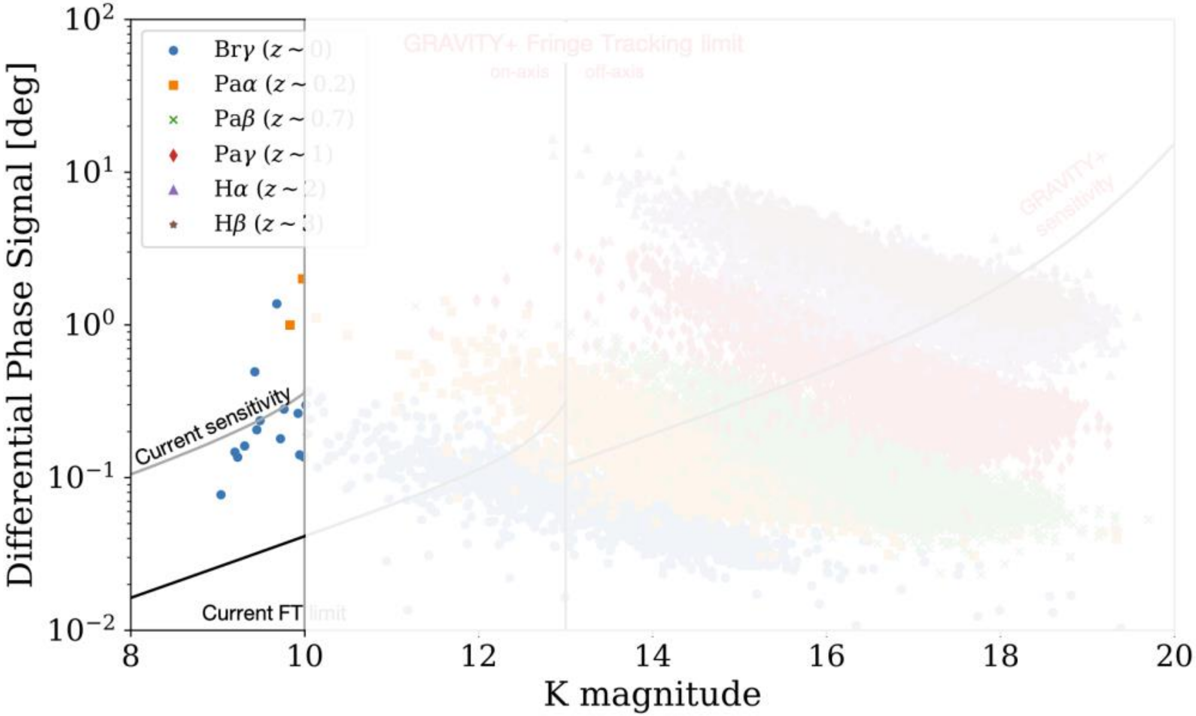

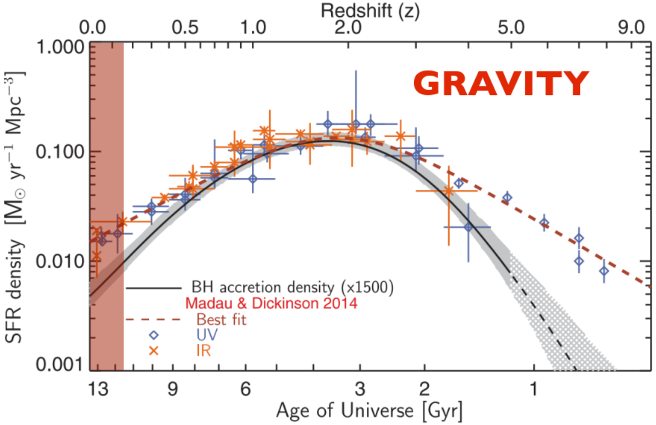

Future Prospects: GRAVITY+

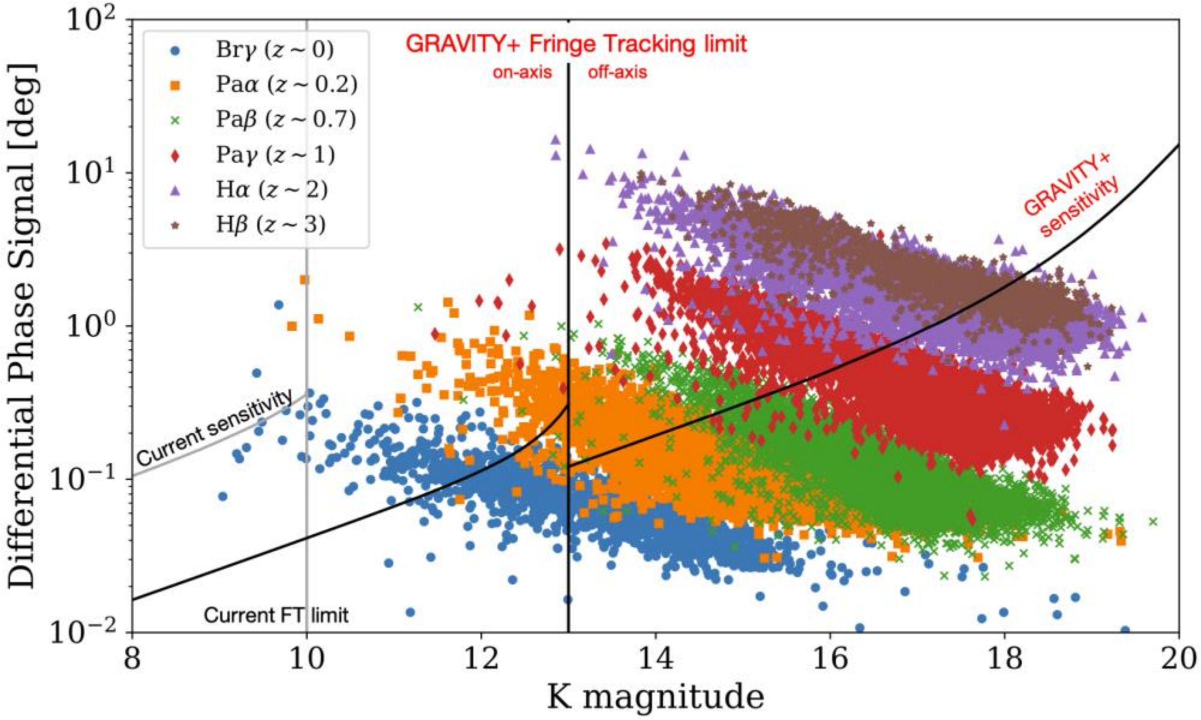

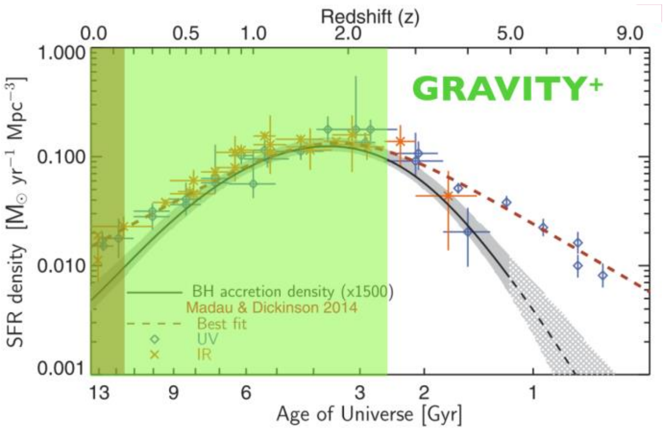

Future Prospects: GRAVITY+

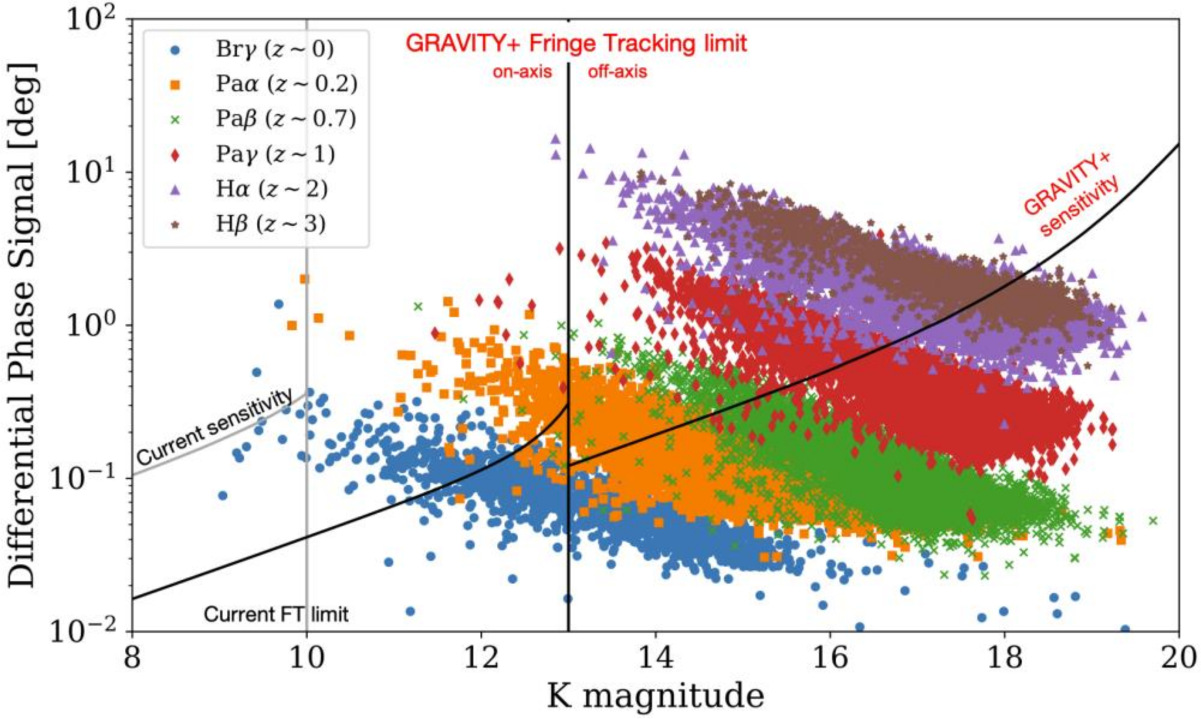

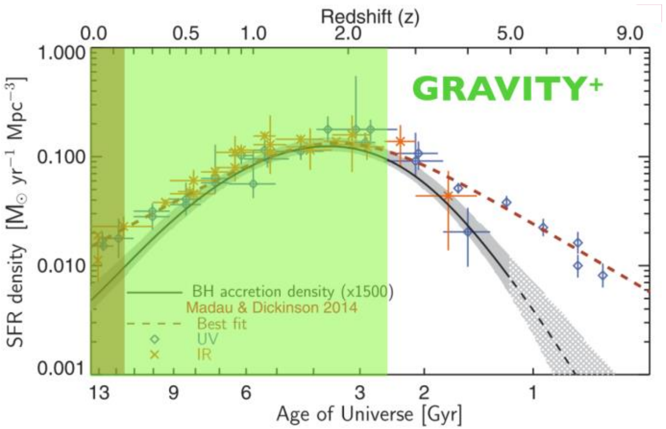

GRAVITY Wide is currently in operation!

Conclusion

Outflow-dominated BLRs

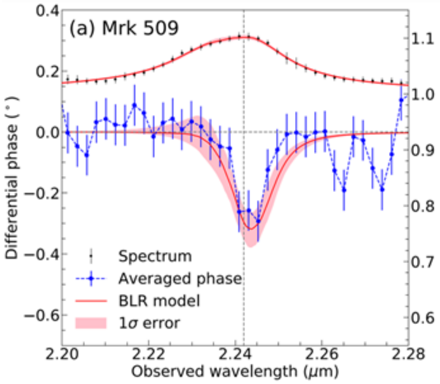

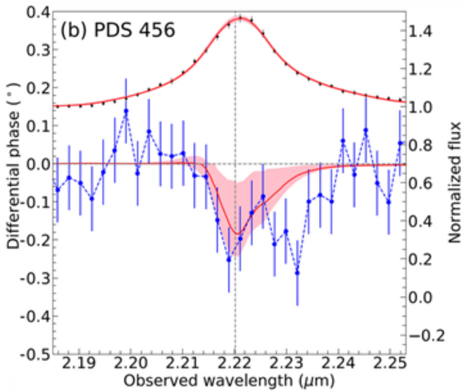

R-L Relation

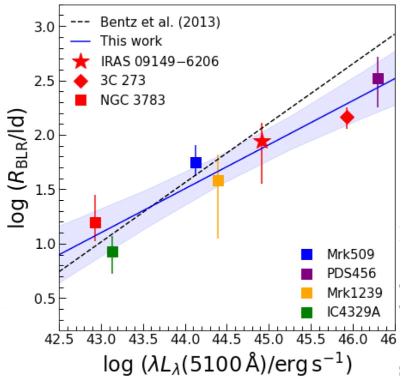

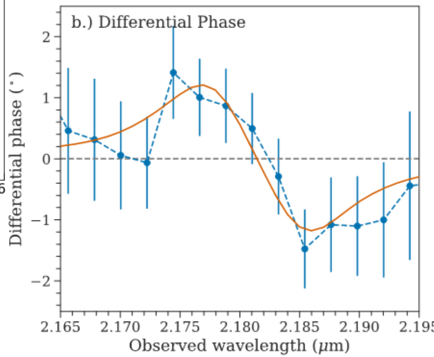

Dynamical mass measurement of a z~2 BH

Virial Factors

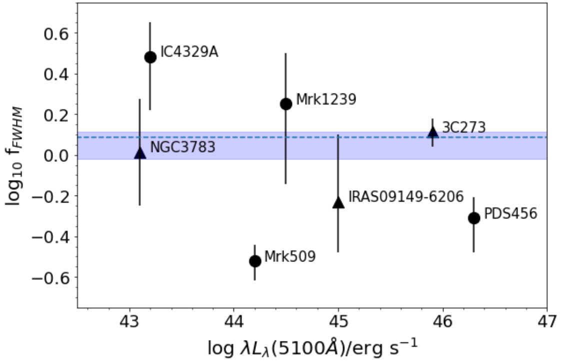

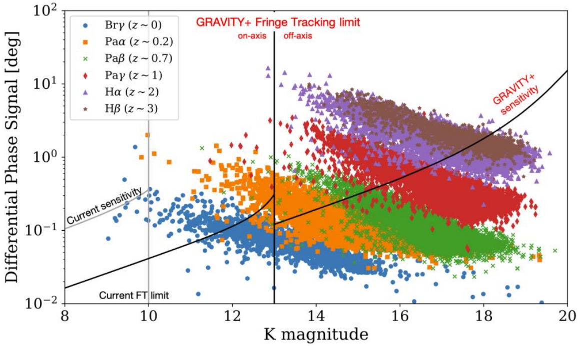

GRAVITY+

Thank you for your attention!

Resolving the BLR and investigating the R-L relation with VLTI/GRAVITY

Back-up slides

BLR offset – AGN luminosity relation

BLR offset has a tight ($p = 0.019$) positive correlation with optical AGN luminosity

Dust continuum radius – AGN luminosity relation (GRAVITY Collab. in prep)

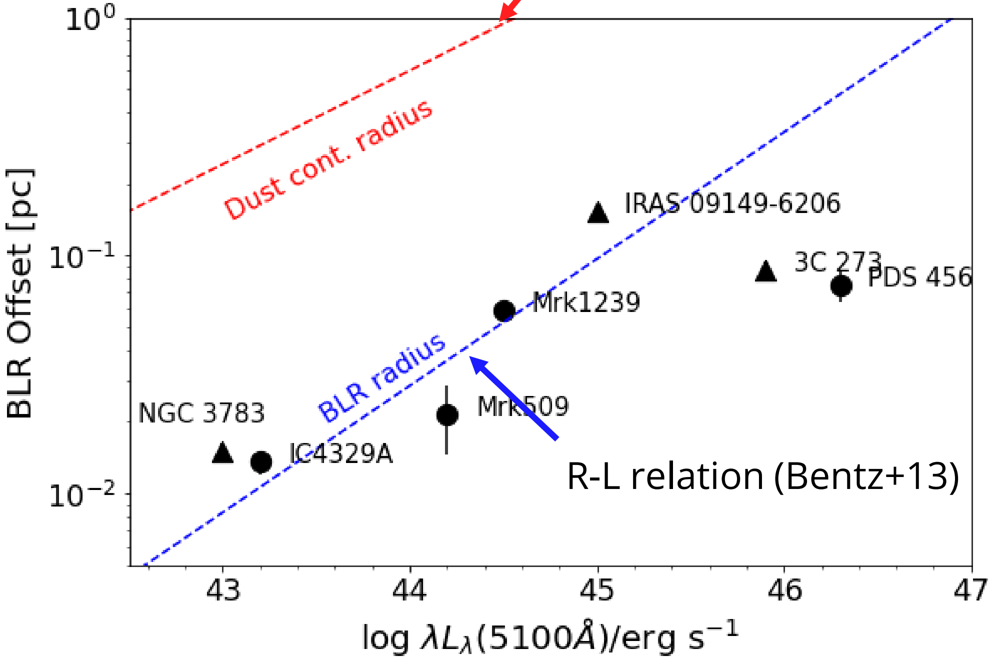

R-L relation (Bentz+13)

BLR Model

BLR Model based on Pancoast+14

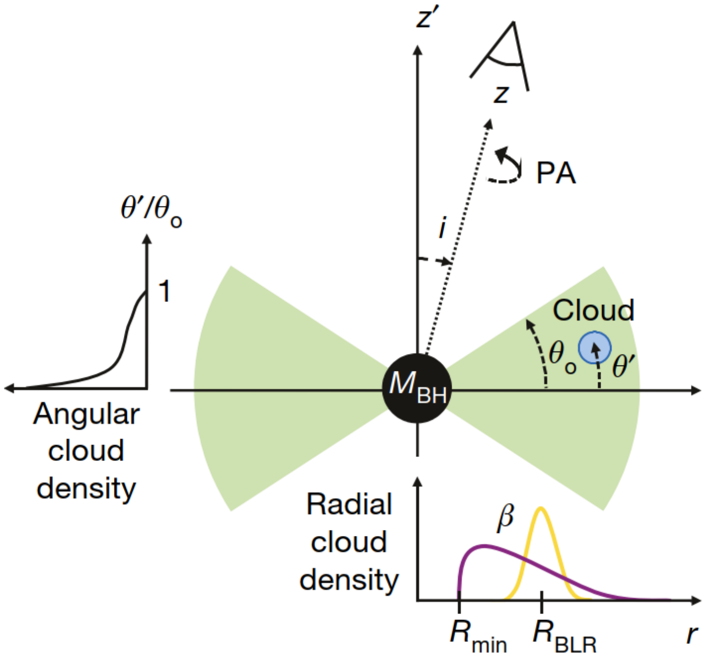

The BLR is a collection of non-interacting clouds encircling the central SMBH.

BLR physical structure described by several parameters that dictate the clouds' position and motion

Table 2. Parameters of the BLR model with definitions, priors, and units where appropriate (all angles are in radians).

$R_{\rm BLR}$	Mean radius of the BLR	LogUniform(10^{-4}, 10 pc)
F	Minimum radius of the BLR in units of $R_{\rm BLR}$	Uniform(0, 1)
β	Unit standard deviation of BLR radial profile	Uniform(0, 2)
$\theta_{\rm o}$	Angular thickness measured from the mid-plane	Uniform(0, $\pi/2$)
i	Inclination angle	Uniform(cos i(0, $\pi/3$))
PA	Position angle of the line of nodes on sky (east of north)	Uniform(0, 2π)
κ	Anisotropy of the cloud emission	Uniform(−0.5, 0.5)
γ	Clustering of the clouds at the edge of the disk	Uniform(1, 5)
ξ	Mid-plane transparency	Uniform(0, 1)
$M_{\rm BH}$	Black hole mass	LogUniform(10^5, 10^{10} $M_\odot$)
$f_{\rm ellip}$	Fraction of clouds in bound elliptical orbits	Uniform(0, 1)
$f_{\rm flow}$	Flag for specifying inflowing or outflowing orbits	Uniform(0, 1)
$\theta_{\rm e}$	Angular location for radial orbit distribution	Uniform(0, $\pi/2$)
$\sigma_{\rho,\rm circ}$	Radial standard deviation for circular orbit distribution	LogUniform(0.001, 0.1)
$\sigma_{\Theta,\rm circ}$	Angular standard deviation for circular orbit distribution	LogUniform(0.001, 1)
$\sigma_{\rho,\rm radial}$	Radial standard deviation for radial orbit distribution	LogUniform(0.001, 0.1)
$\sigma_{\Theta,\rm radial}$	Angular standard deviation for radial orbit distribution	LogUniform(0.001, 1)
$\sigma_{\rm turb}$	Normalised standard deviation of turbulent velocities	LogUniform(0.001, 0.1)
$\lambda_{\rm emit}$	Central wavelength of the emission line	Norm(2.2896, 0.002 μm)
$f_{\rm peak}$	Peak flux of the normalised line profile	Uniform(0.05, 0.065)
$(x_{\rm o}, y_{\rm o})$	Offset of the origin of the BLR	Uniform(−1, 1 mas)

Derivation of BLR Offset Model

- Let P_{cont} (orig. continuum photocenter) and P_{BLR} (BLR photocenter) at the origin = (0,0), and similar to the center of mass formula:

$$P_{cont} = \frac{\Sigma w_i r_i}{\Sigma w_i}$$

where w_i = flux (weight) of individual clouds.

- P'_{cont} = new continuum photocenter

- If the hot dust is composed of two semicircular annuli with different fluxes, W_l and W_r, we have:

$$P'_{cont} = \frac{\Sigma w_l r_l + \Sigma w_r r_r}{\Sigma w_l + \Sigma w_r}$$

$$= \frac{1}{\pi(W_l+W_r)}\left(W_l R_{dust}\int_{\frac{\pi}{2}}^{\frac{3\pi}{2}} cos\theta d\theta + W_r R_{dust}\int_{-\frac{\pi}{2}}^{\frac{\pi}{2}} cos\theta d\theta\right)^*$$

$$= \frac{2(W_r R_{dust} - W_l R_{dust})}{\pi(W_l + W_r)} = \frac{2R_{dust}(W_r - W_l)}{\pi(W_l + W_r)}$$

*Because r_r = -r_l
(symmetry in y-axis)

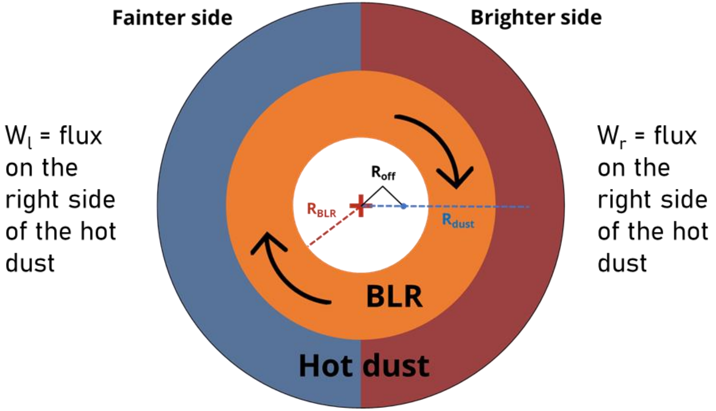

Since $R_{off} = P'_{cont} - P_{BLR} = P'_{cont}$, we have:

$$R_{off} = \frac{1}{\pi}\left(\frac{W_r - W_l}{W_r + W_l}\right)2R_{dust}$$

$$\rightarrow \boxed{f = \frac{R_{off}}{R_{dust}} = \frac{2}{\pi}\frac{W_r - W_l}{W_r + W_l}}$$

To calculate W_r/W_l, we have:

$$\boxed{\frac{W_r}{W_l} = \frac{2+\pi f}{2-\pi f}}$$

Differential Phase

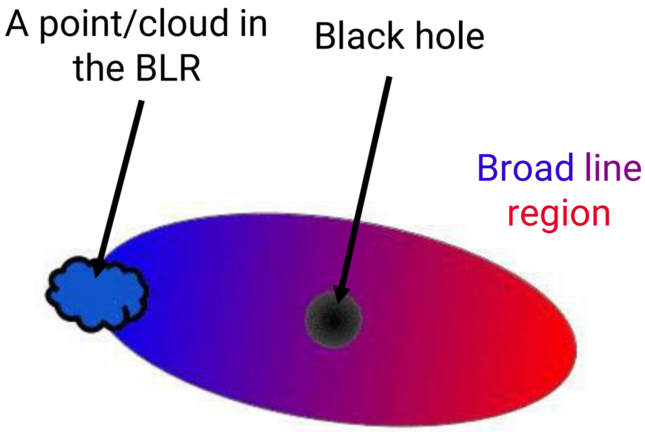

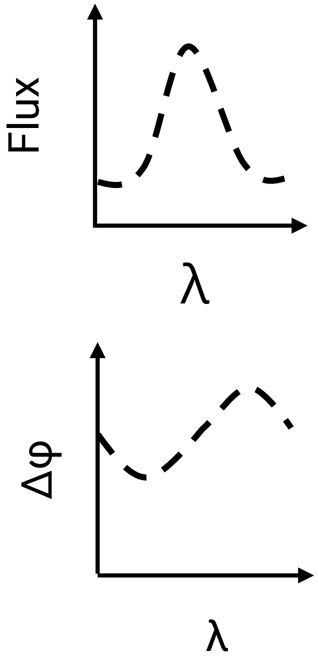

Differential phase (Δφ) – relative position of the fringe phase along wavelengths (measured wrt the hot dust continuum photocenter)

Differential Phase

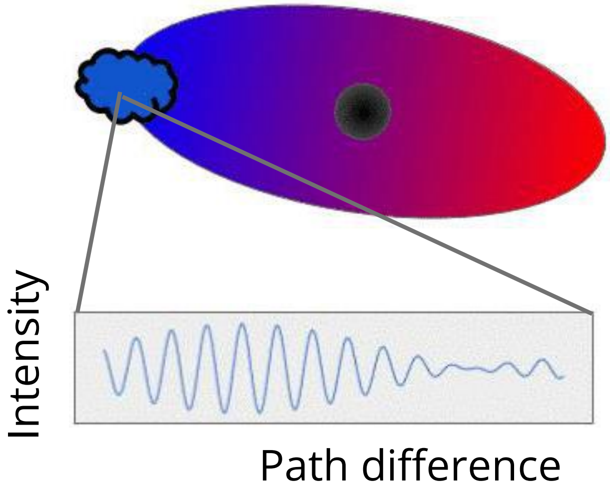

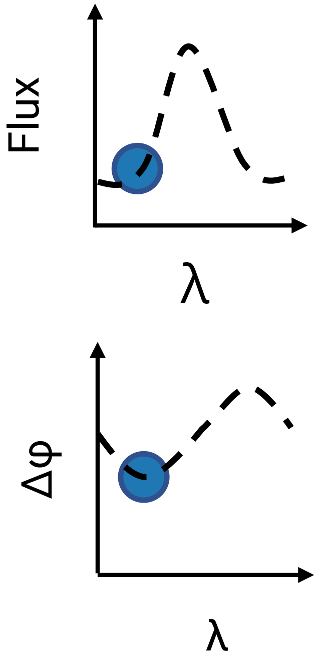

Differential phase (Δφ) – relative position of the fringe phase along wavelengths (measured wrt the hot dust continuum photocenter)

Differential Phase

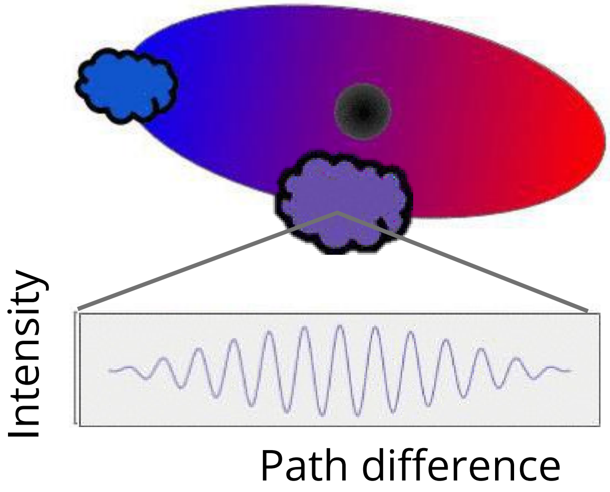

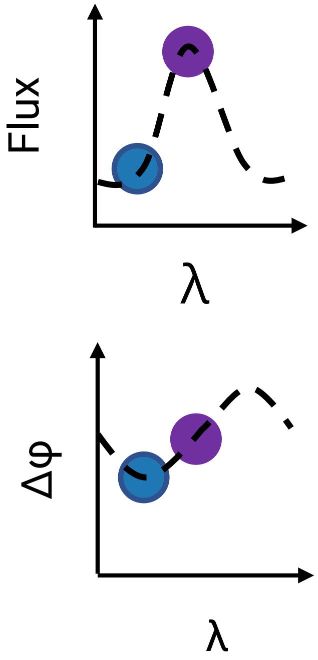

Differential phase (Δφ) – relative position of the fringe phase along wavelengths (measured wrt the hot dust continuum photocenter)

Differential Phase

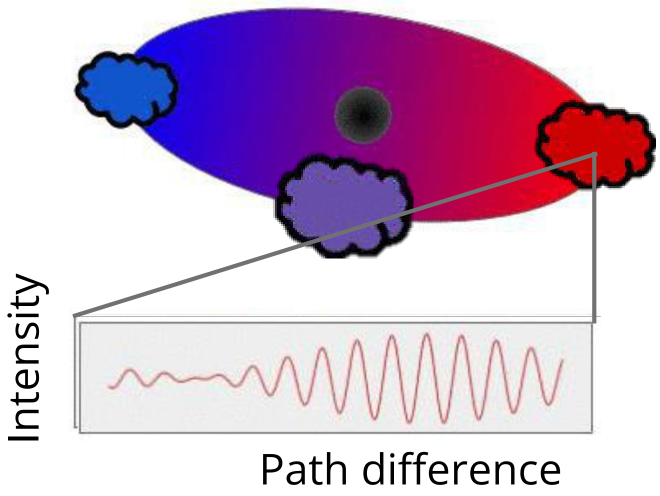

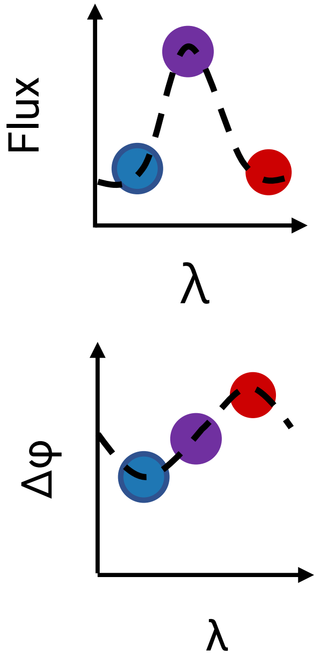

Differential phase (Δφ) – relative position of the fringe phase along wavelengths (measured wrt the hot dust continuum photocenter)

Differential Phase

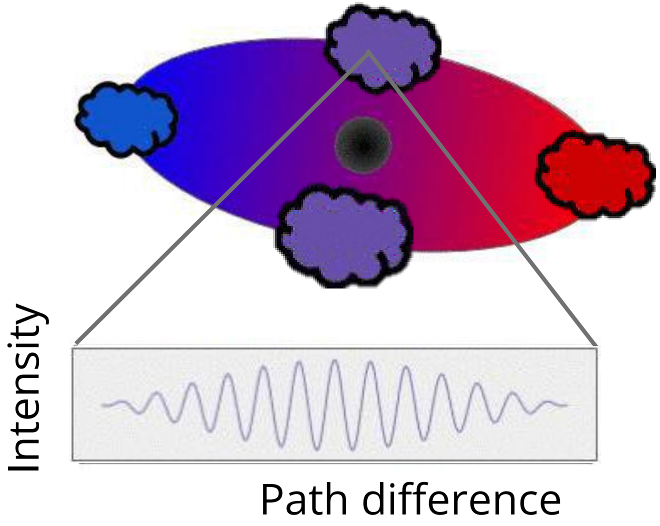

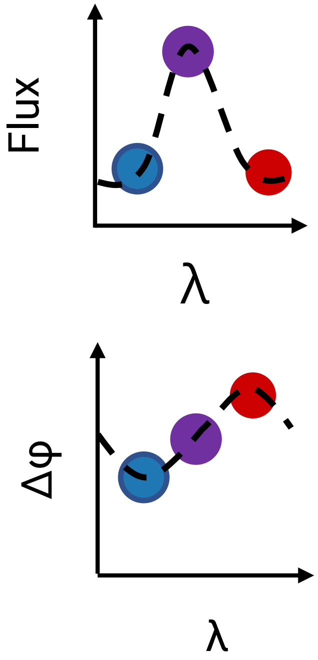

Differential phase (Δφ) – relative position of the fringe phase along wavelengths (measured wrt the hot dust continuum photocenter)

Differential Phase

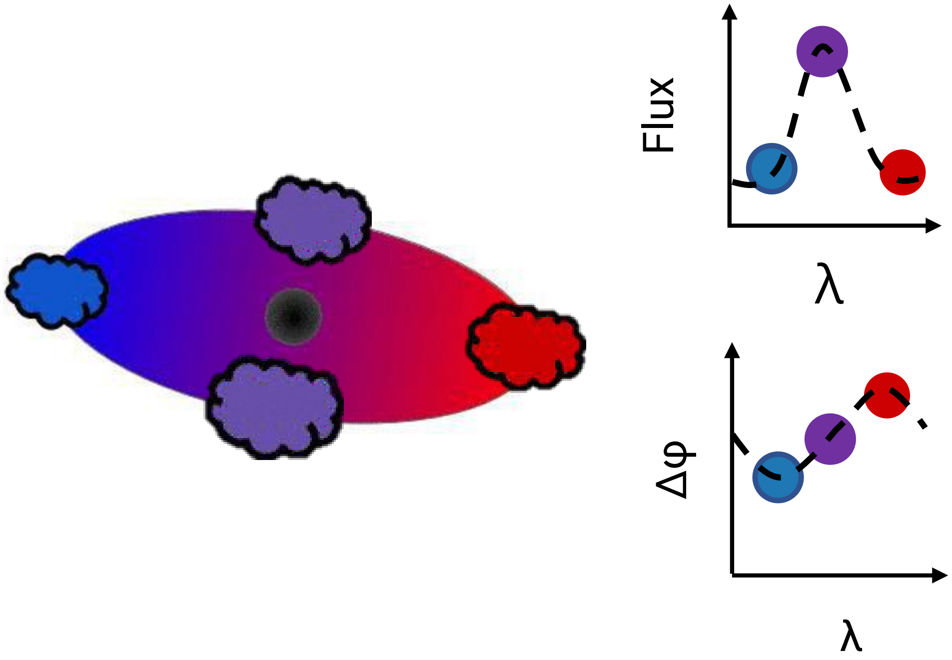

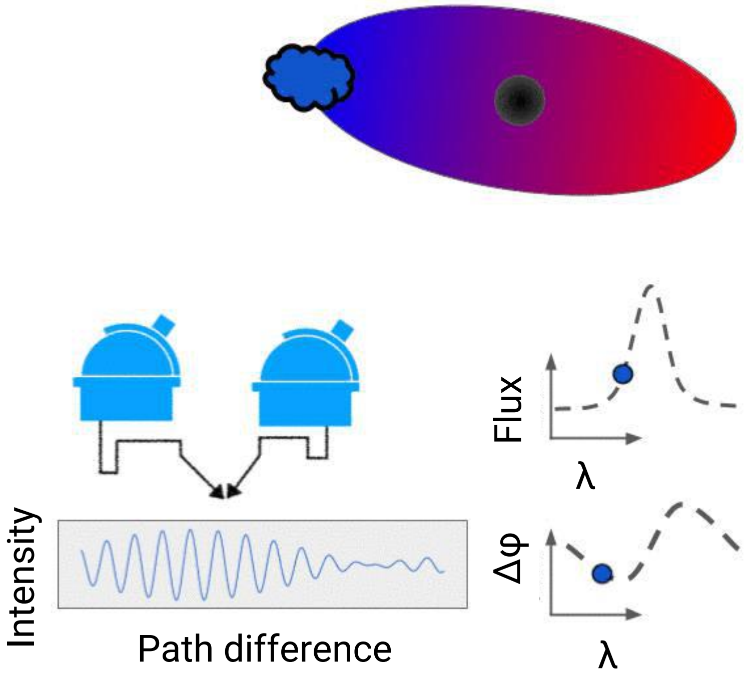

Differential Phase

However, the observed differential phase could be different from the typical S-shaped profile:

Observed AGN emission = Continuum emission from hot dust + Line emission from BLR

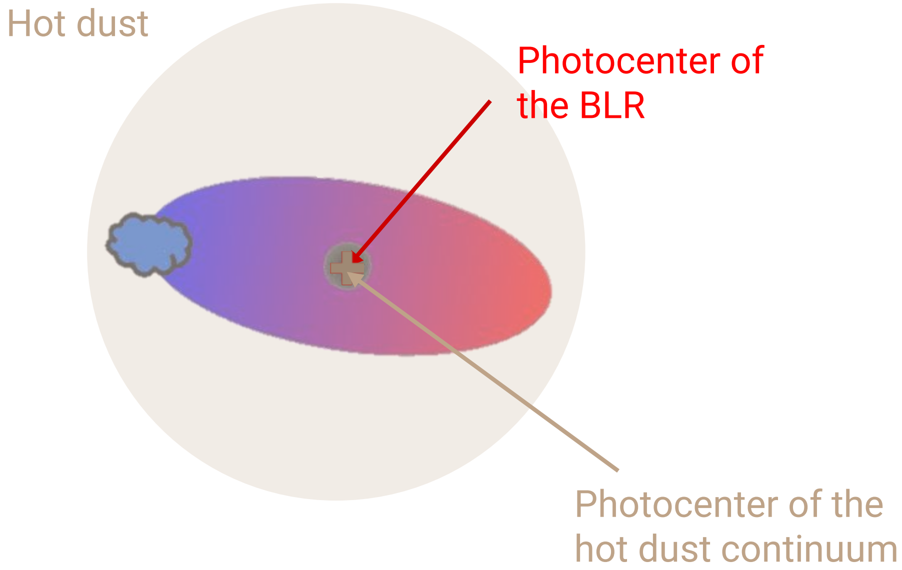

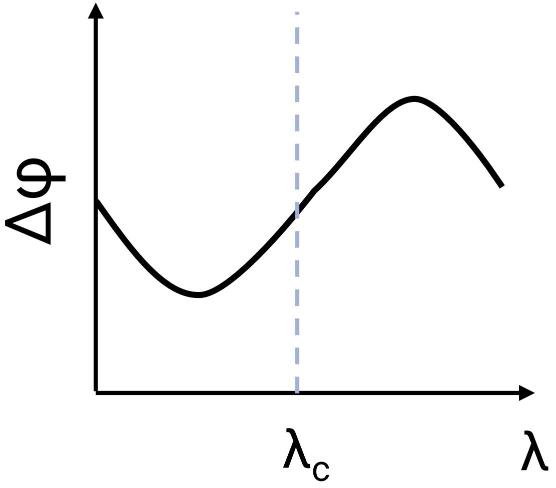

Differential Phase

However, the observed differential phase could be different from the typical S-shaped profile:

Observed AGN emission = Continuum emission from hot dust + Line emission from BLR

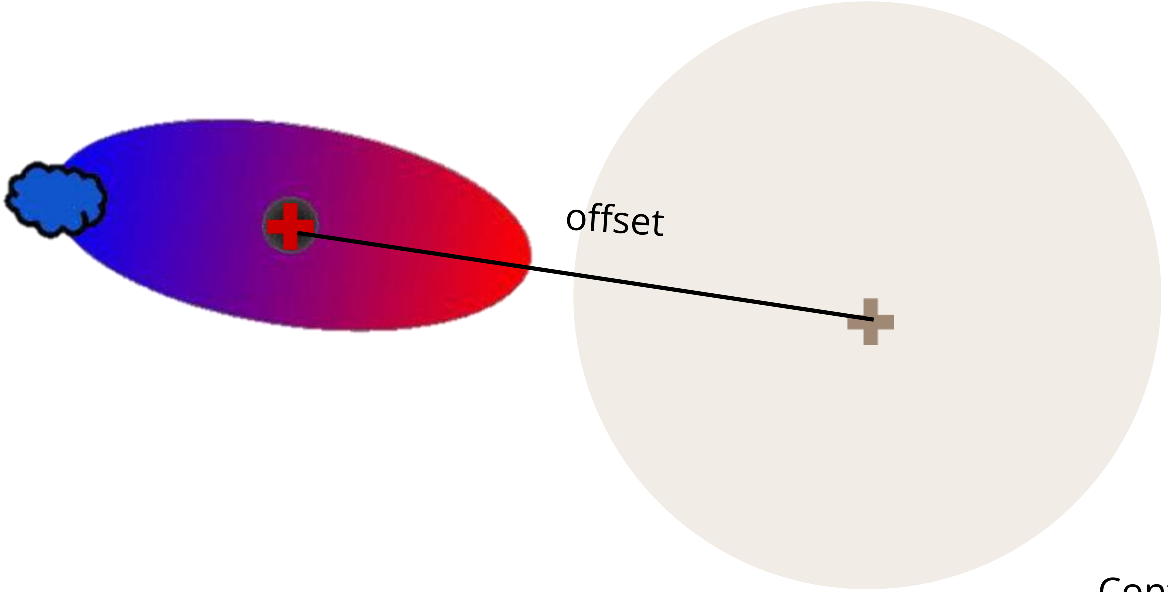

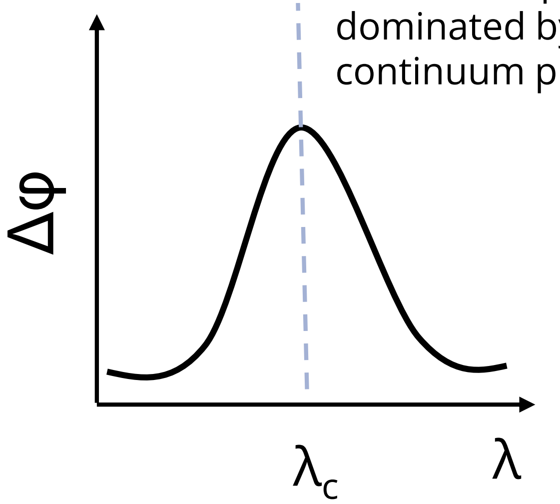

Differential phase dominated by the continuum phase

<u>Continuum phase must be subtracted later</u>

Asymmetries in the BLR Model

Parameters that can reproduce asymmetric differential phase signals

BLR emission anisotropy (κ)

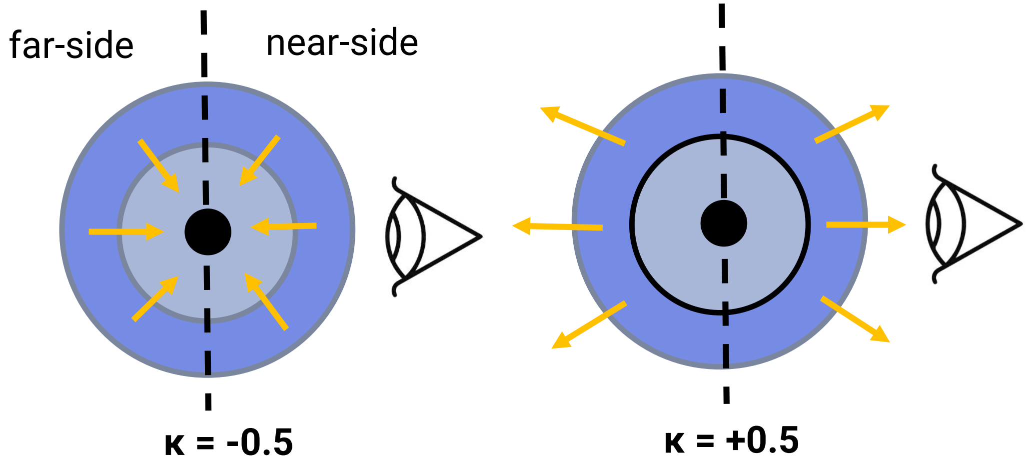

$$w = 0.5 + \kappa \cos \varphi,$$

where w = weighting/relative strength of a cloud's emission
φ = angle b/w LoS and BH

κ = -0.5 → preferential emission from the far side of the BLR from the observer

κ = +0.5 → preferential emission from the near side of the BLR from the observer

Asymmetries in the BLR Model

Parameters that can reproduce asymmetric differential phase signals

BLR mid-plane transparency (ξ)

$\xi = 1 \rightarrow$ no obscuration

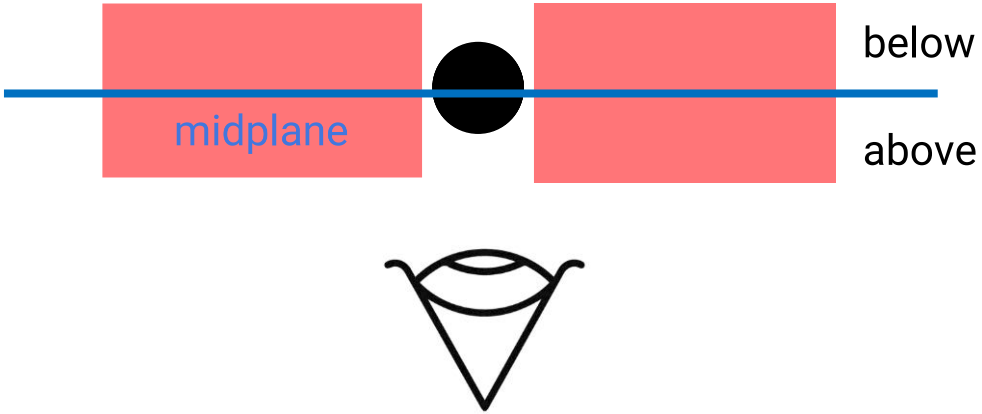

Asymmetries in the BLR Model

Parameters that can reproduce asymmetric differential phase signals

BLR mid-plane transparency (ξ)

$\xi = 1 \rightarrow$ no obscuration
$\xi = 0 \rightarrow$ complete obscuration

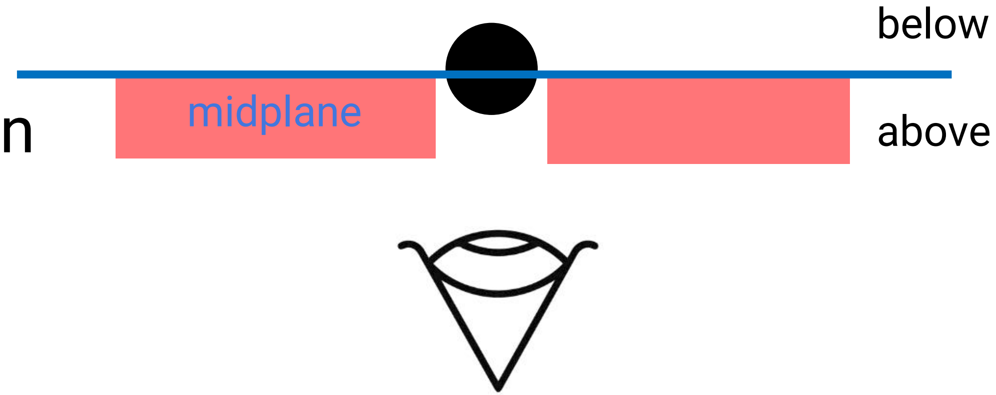

BLR Asymmetry of Mrk 509

κ

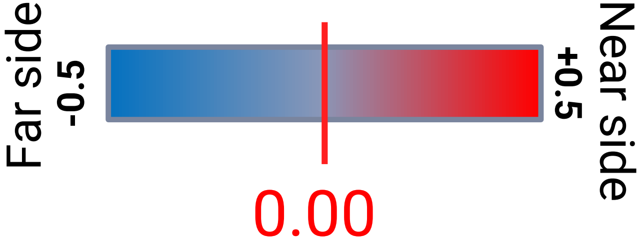

Larger clouds → larger κ
Smaller clouds → smaller κ

ξ

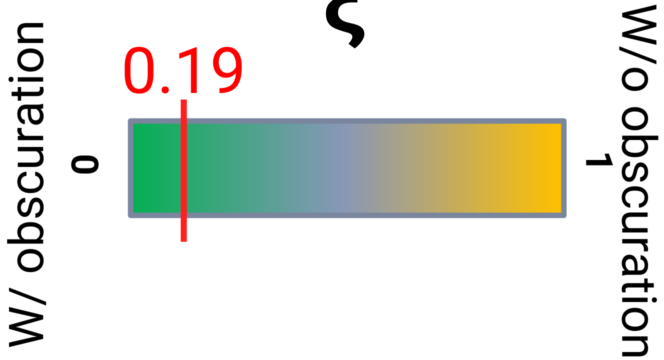

More clouds below midplane → w/o obscuration
Fewer clouds below midplane → with obscuration

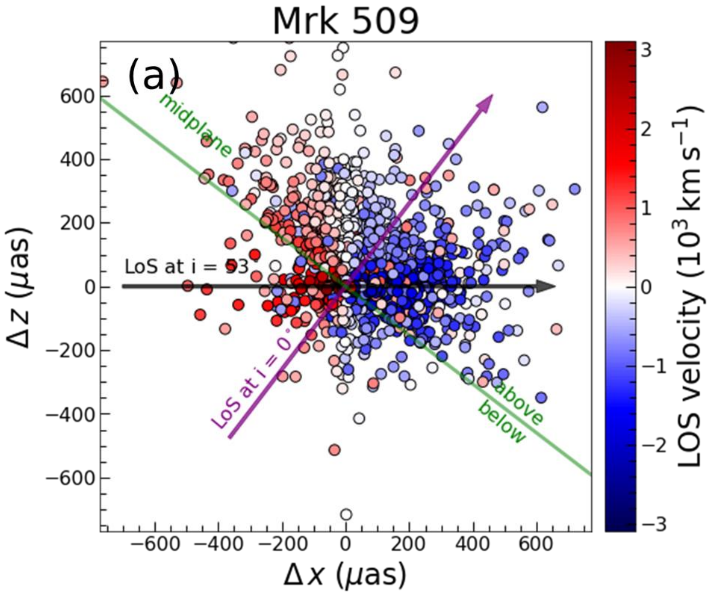

BLR Asymmetry of PDS 456

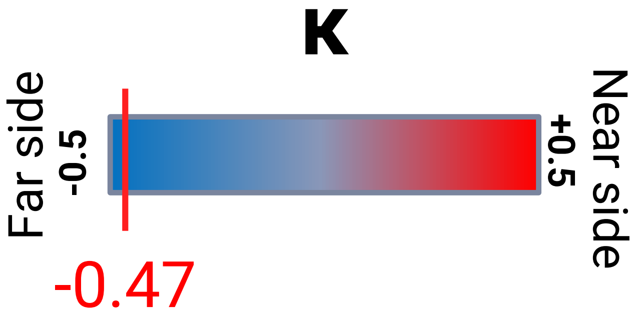

Larger clouds → larger κ
Smaller clouds → smaller κ

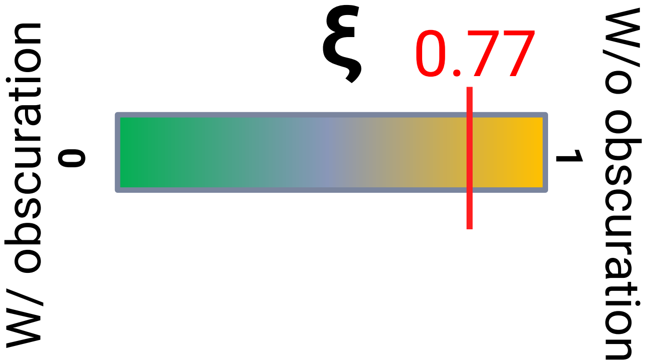

More clouds below midplane → w/o obscuration
Fewer clouds below midplane → with obscuration

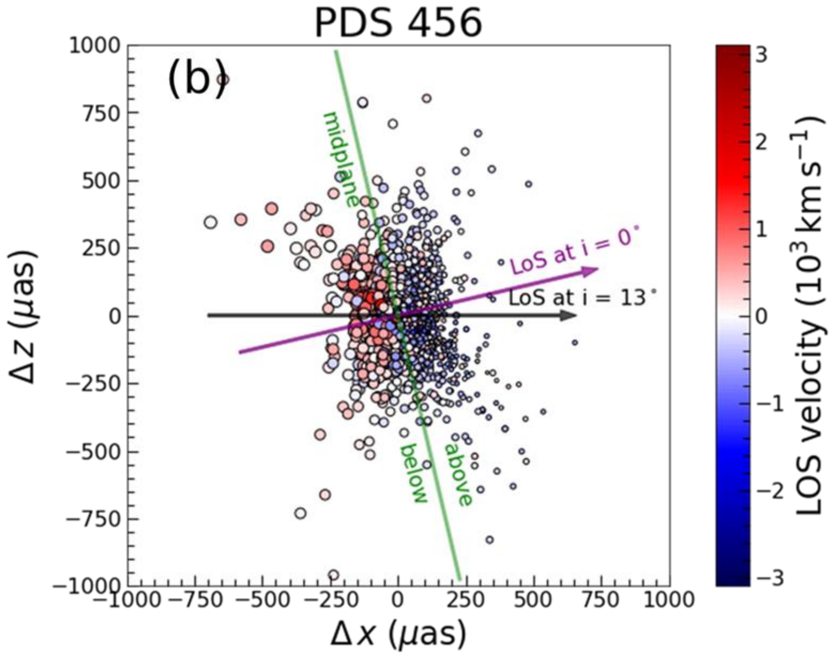

BLR Fitting Results for all 4 AGNs

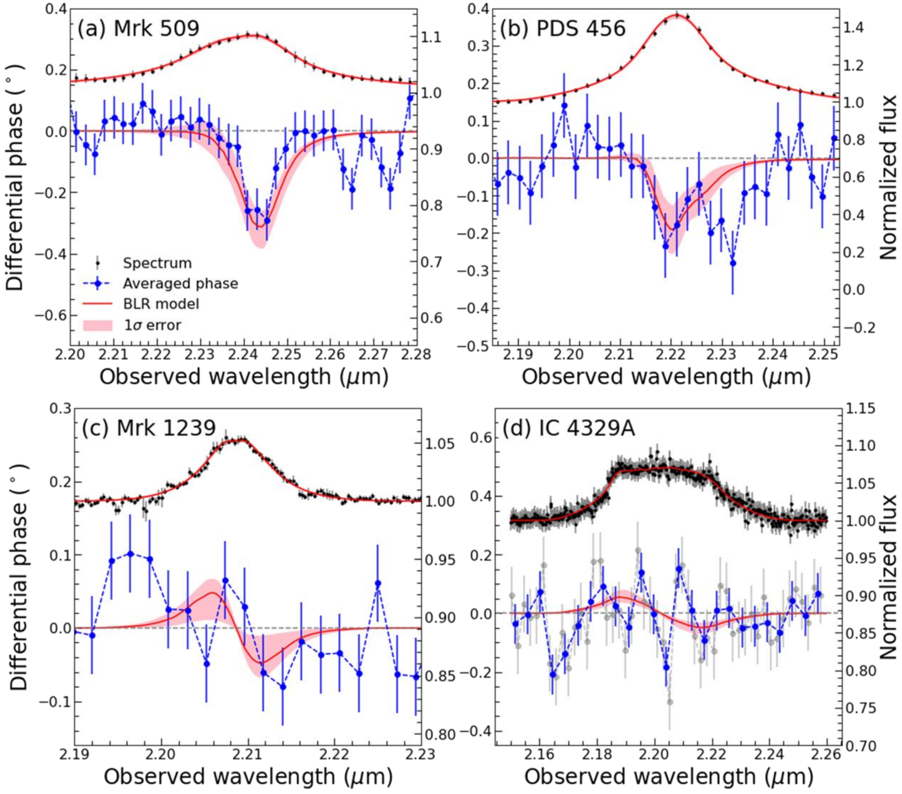

Target	log R_{BLR} [ld]	log M_{BH} [$M_\odot$]
Mrk 509	$1.74^{+0.16}_{-0.12}$	$7.74^{+0.21}_{-0.15}$
PDS 456	$2.38^{+0.19}_{-0.27}$	$8.02^{+0.23}_{-0.28}$
Mrk 1239	$1.56^{+0.24}_{-0.53}$	$7.22^{+0.39}_{-0.68}$
IC 4329A	$0.92^{+0.14}_{-0.20}$	$8.18^{+0.18}_{-0.22}$

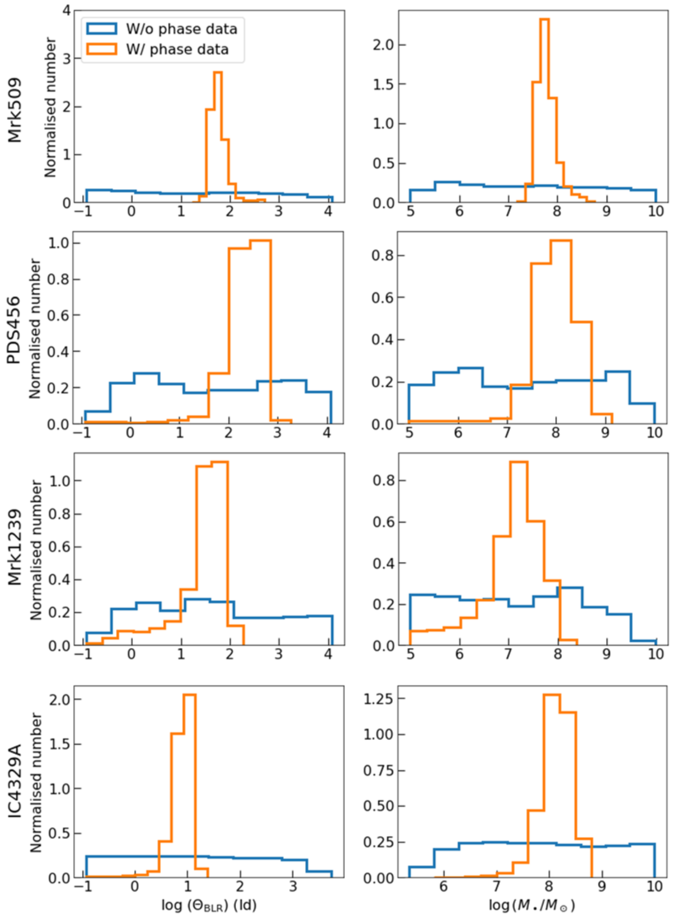

Importance of Differential Phase in BLR Fitting

Figure shows posterior distribution of BLR radius (left column) and BH mass (right column) with (orange histogram) and without (blue histogram) phase data.

Posterior distribution derived with phase data has much clearer peaks → better fitting

Phase signals of Mrk 1239 and IC 4329A act as a limit

Are the differential phase spectra of Mrk 1239 and IC 4329A and their corresponding model-derived differential phase spectra reliable?

As a check, we investigate the expected range of phase signals for Mrk 1239 and IC 4329A fitting only their flux spectra.

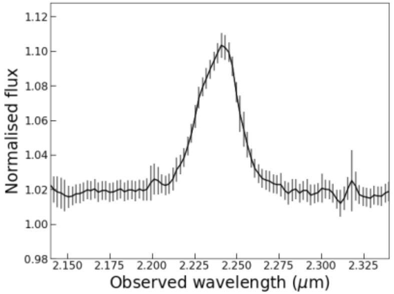

Data flux spectrum

BLR Model based on Pancoast+14

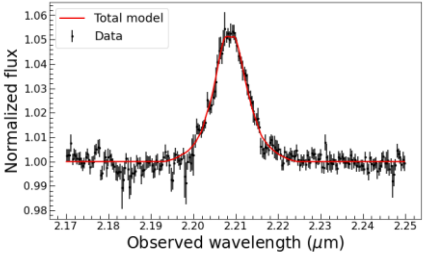

Model flux spectrum

Phase signals of Mrk 1239 and IC 4329A act as a limit

Since we have the uv-coordinates of the baselines ($\boldsymbol{u}$) and we can calculate for the centroids corresponding to each spectral channel ($\boldsymbol{x_{BLR,\lambda}}$), we can calculate for the differential phase in each spectral channel ($\Delta\phi_\lambda$).

$$\Delta\phi_\lambda = -2\pi\left(\frac{f_\lambda}{1+f_\lambda}\right)\boldsymbol{u}\cdot\boldsymbol{x_{BLR,\lambda}}$$

During calculation, the BH masses of each resulting best-fit model is fixed to their minimum and maximum values based on previous literature.

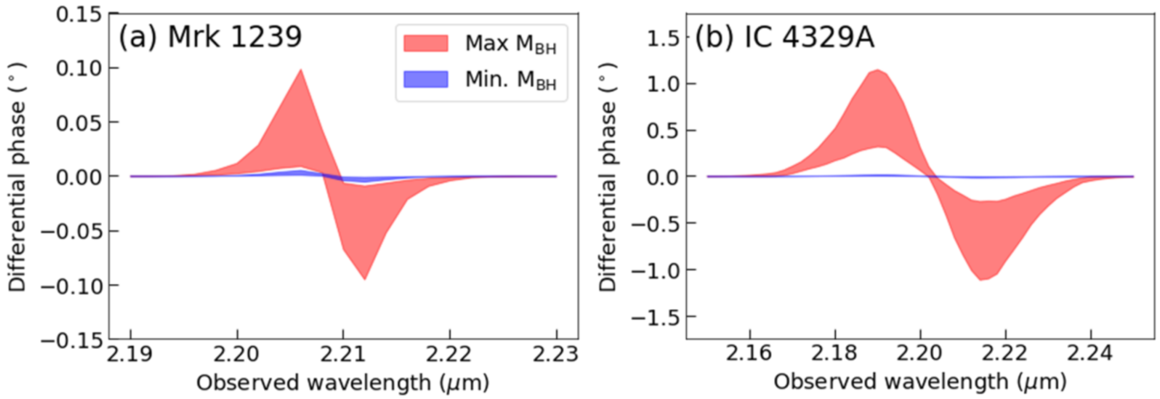

Phase signals of Mrk 1239 and IC 4329A act as a limit

Since the BLR size, inclination angle, and BH mass are degenerate, the expected phase signals will also reflect the possible inclination angles and BLR sizes for these objects

Fitting only the flux spectrum gives a wide range of possible BLR sizes/inclination angles.

Weak phase signals of Mrk 1239 and IC 4329A act as a constraint.

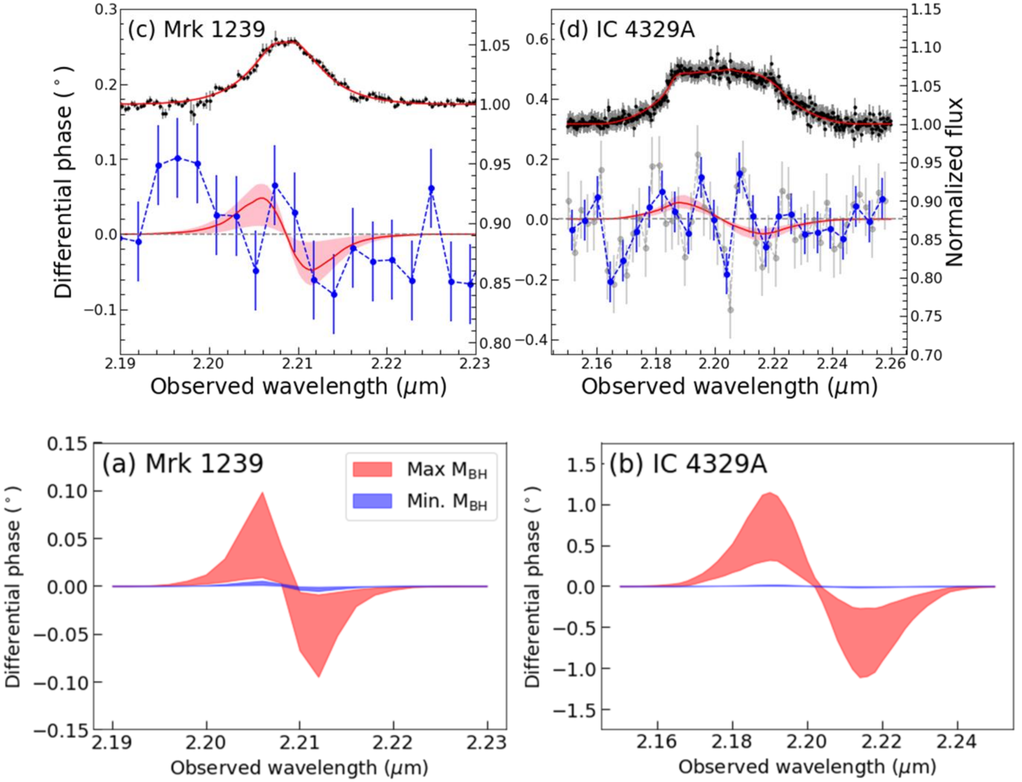

M-σ relation

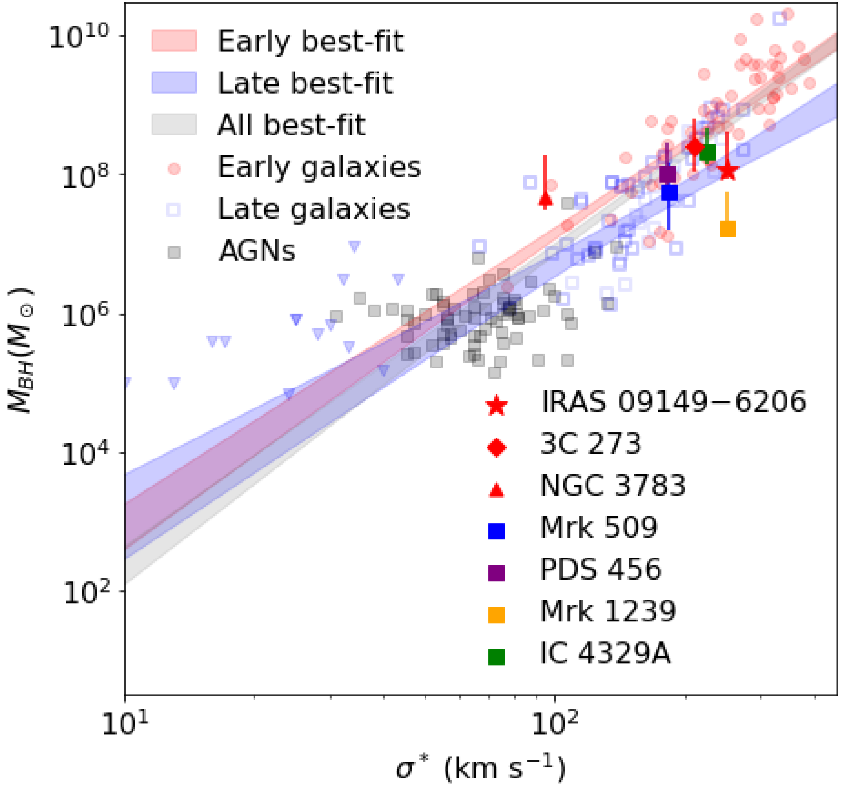

GRAVITY AGNs on the upper edge of low-mass AGNs from Xiao+11

Also consistent with other AGNs within uncertainties

Sample Selection for GRAVITY-AGN Project

1. Nuclear $K \lesssim 10$, $V \lesssim 15$ mag
2. Type 1 (Sy1/QSO with broad Paα or Brγ lines)
3. Large predicted BLR phase signals
4. Spanning the full range of AGN luminosity
5. Spanning a full range of system position angle or BLR kinematics information (either from velocity-resolved RM, MIR interferometry, radio, and/or high-resolution narrow emission line observations)

Photocenter Fitting

$$\Delta\phi_\lambda = -2\pi \left(\frac{f_\lambda}{1+f_\lambda}\right) \boldsymbol{u} \cdot \boxed{\boldsymbol{x_{BLR,\lambda}}}$$

Differential Phase

Photocenter of each spectral channel

Normalized flux

uv coordinate of each baseline

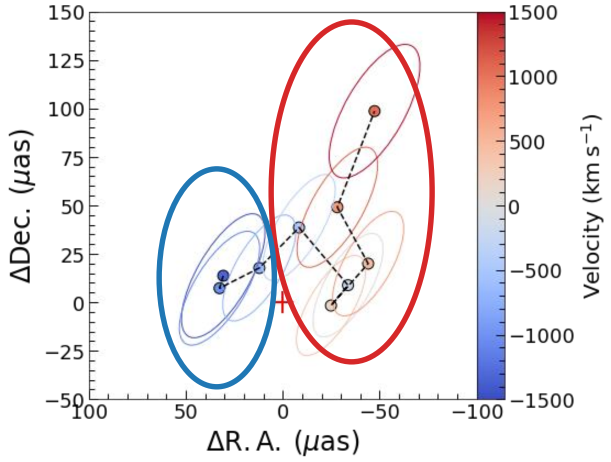

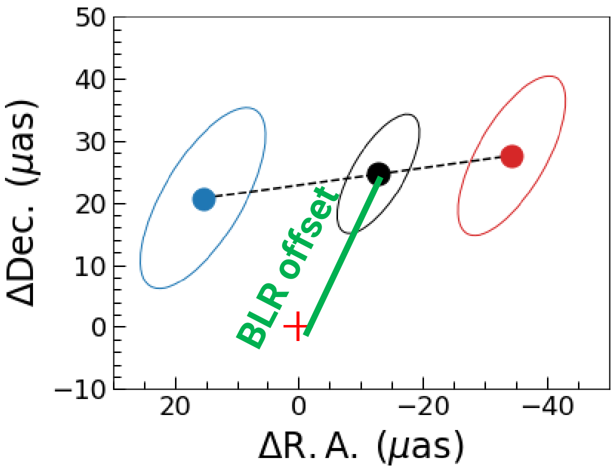

Origin of BLR offset

Possible reason: Asymmetric emission from hot dust

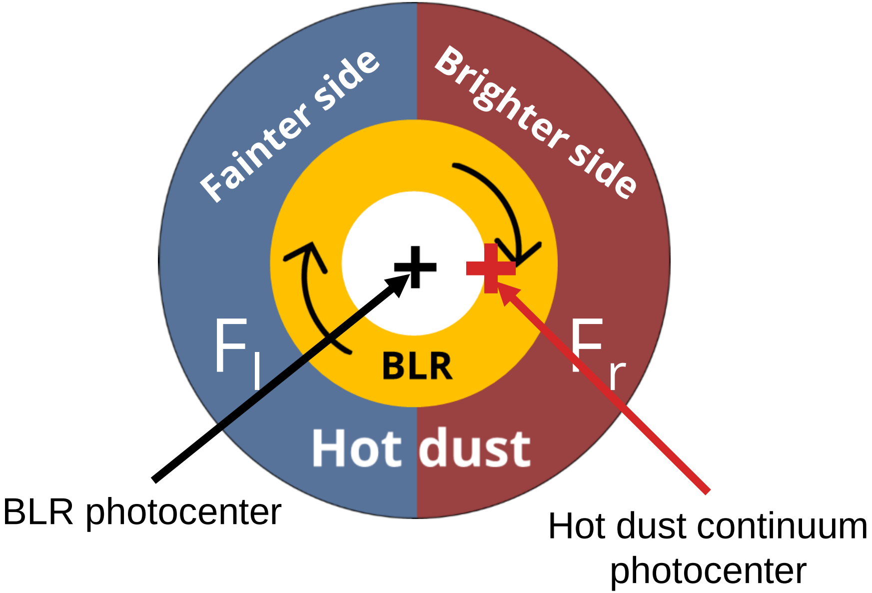

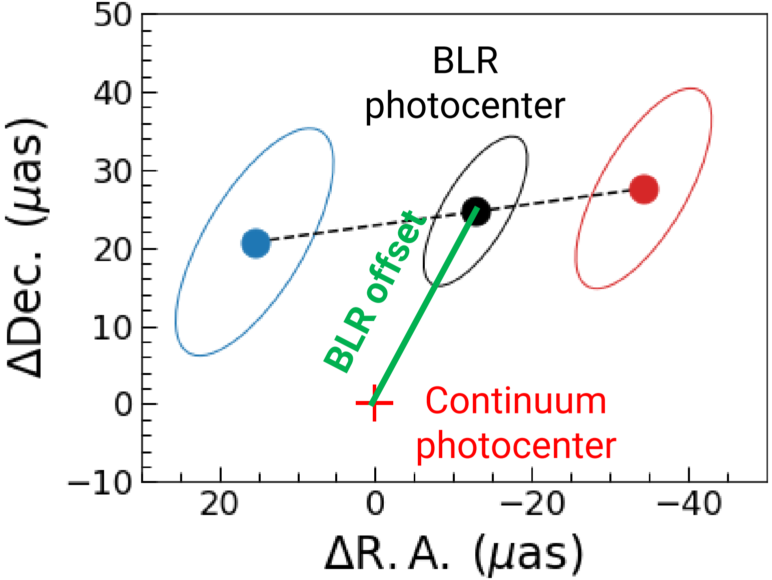

Origin of BLR offset

Possible reason: Asymmetric emission from hot dust

$$\frac{F_r}{F_l} = \frac{2+\pi f}{2-\pi f} \qquad f = \frac{R_{off}}{R_{dust}}$$

On average, the hot dust of GRAVITY-observed AGNs emit anisotropically, **with one side ~33% brighter than the other**.

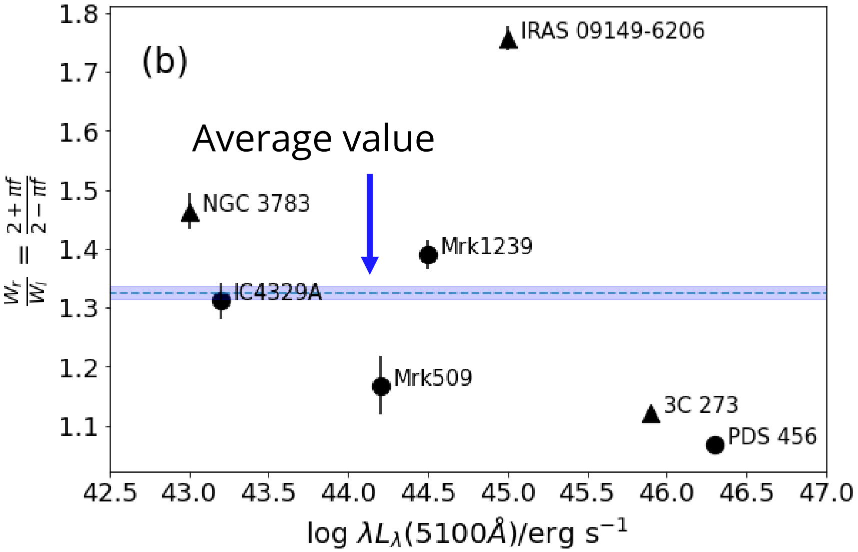

GRAVITY-Wide

GRAVITY: Fringe tracker (FT) source and science target (SC) within VLTI's FoV (~2")

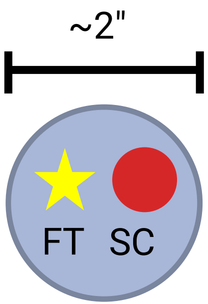

GRAVITY Wide: Wide-angle off-axis fringe tracking → separation b/w FT and SC up to ~30"

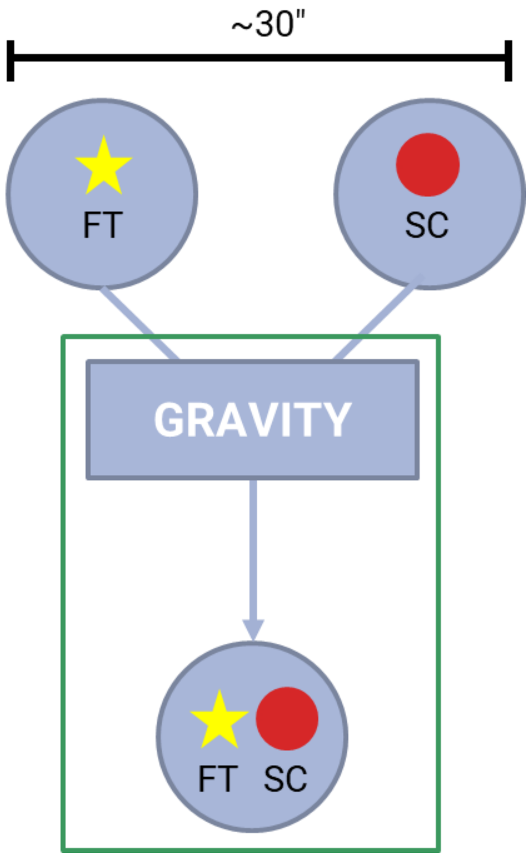

GRAVITY+

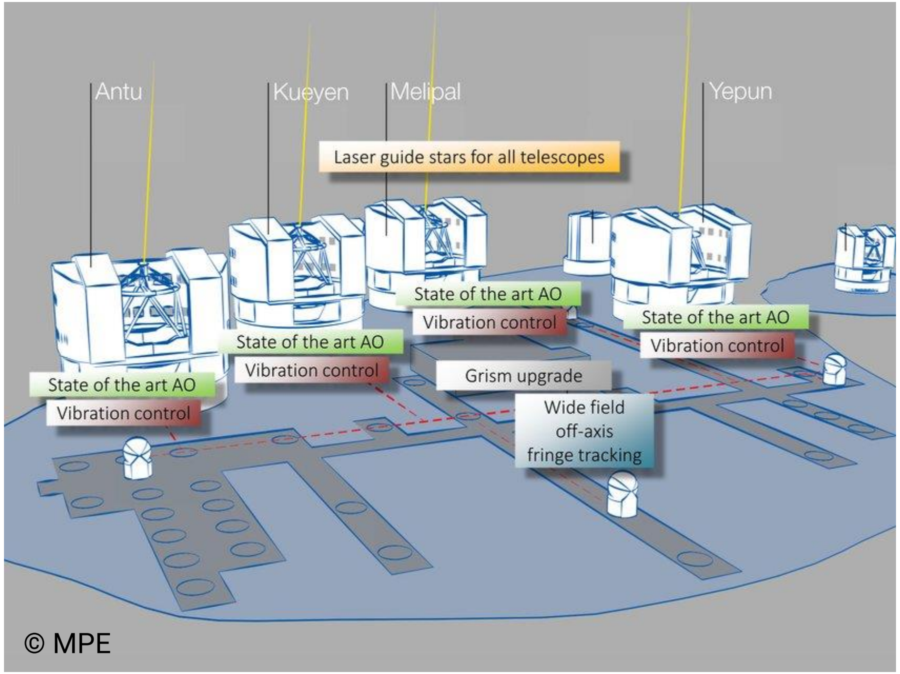

- Laser guide stars for all telescopes
- Wide-field off-axis fringe tracking (GRAVITY Wide)
- Fainter (K = 22 mag) targets

Offset of BLR sizes from classical R-L relation vs. Eddington ratio